World Journal of Advanced Research and Reviews
eISSN: 2581-9615 CODEN (USA): WJARAI
Cross Ref DOI: 10.30574/wjarr
Journal homepage: https://wjarr.com/

(Research Article)

Check for updates

DESIGN AND IMPLEMENTATION OF AN IOT-ENABLED AUTOMATIC POWER FACTOR CORRECTION SYSTEM USING ESP8266

Anurag Singh * and Yatresh Mishra

Department of Electronics Engineering, Kamla Nehru Institute of Technology, Sultanpur – 228118, India.
* Corresponding Author

ORCID Details
Anurag Singh: https://orcid.org/0009-0005-0440-4322
Yatresh Mishra: https://orcid.org/0009-0005-2138-1812

World Journal of Advanced Research and Reviews, 2026, 31(02), 1102–1113

Publication history: Received on 03 July 2026; revised on 15 August 2026; accepted on 17 August 2026

Article DOI: https://doi.org/10.30574/wjarr.2026.31.2.2131

ABSTRACT

Low power factor in inductive electrical loads increases line current, reactive-power demand, voltage drop, and system losses. This paper presents a low-cost Automatic Power Factor Correction (APFC) prototype built around an ESP8266 controller, an ACS712 current sensor, relay-switched capacitor stages, a 16 x 2 LCD, and the Blynk IoT platform. The prototype supports local and remote visualization of current, estimated power factor, capacitor status, load status, and automatic/manual operating modes. In the supplied firmware, power factor is estimated from known load states and programmed correction increments rather than being directly calculated from simultaneous voltage-current phase measurement. The control algorithm applies current thresholds, a three-reading stability condition, and a five-second inter-stage delay to reduce relay chatter and capacitor inrush effects. For the transformer-only load model, the programmed power factor increases from 0.62 without compensation to 0.73 with the first capacitor stage and to 0.96 with both stages. The original interface records show representative low-power-factor and corrected states of 0.62 and 0.96, respectively. The work demonstrates the feasibility of an IoT-assisted APFC teaching prototype while also identifying the need for calibrated voltage sensing, zero-crossing/phase-angle measurement, and controlled meter-based experiments before industrial deployment.

Keywords: Automatic power factor correction; ESP8266; Capacitor bank; ACS712; Relay control; Blynk IoT; Reactive power compensation

1 INTRODUCTION

Electrical systems containing motors, transformers, fluorescent-lighting chokes, and other inductive loads require both active and reactive power. The resulting lag between current and voltage reduces the power factor, increases current for a given active-power demand, and contributes to additional conductor losses and voltage drop [1]-[4]. Manual or fixed capacitor compensation may improve the operating point, but it cannot respond reliably to variable load conditions and may produce under-compensation or over-compensation.

Automatic Power Factor Correction (APFC) systems address this problem by observing the electrical operating state and switching suitable capacitor steps in parallel with the load. Microcontroller-based APFC is attractive for educational and small-scale applications because sensing, decision logic, display, and communication can be integrated into a compact platform. Earlier work has established the importance of improved power-quality converters, instantaneous reactive-power compensation, and controlled power-factor-correction techniques [5]-[8].

The project reported here develops an IoT-enabled APFC prototype using an ESP8266, current sensing, relay switching, capacitor stages, resistive and inductive demonstration loads, a local LCD, and Blynk web/mobile dashboards. The primary contribution is the integration of automatic staged compensation with remote supervision and manual override in a low-cost demonstrator. The paper retains the original project figures and numerical settings while reorganizing the material into a research-paper structure.

A scientifically important distinction is maintained throughout this paper: although the conceptual block diagram includes voltage and current sensing, the supplied implementation code explicitly states that no voltage sensor or zero-crossing detector is used. Consequently, the displayed power factor is a firmware estimate based on selected load states and capacitor states, not a direct laboratory measurement of phase angle. This limitation is considered in the discussion and future work.

2 RELATED WORK

Singh et al. surveyed single-phase improved-power-quality AC-DC converter families and emphasized input-current shaping and high power factor as central power-quality objectives [5]. Akagi et al. introduced instantaneous reactive-power compensation using switching devices, which became foundational for real-time compensator design [6]. Redl and Balogh examined power-factor correction in rectifier circuits using inductive and capacitive elements [7]. Chattopadhyay et al. presented a broader treatment of electric power-quality phenomena and assessment methods [8].

Conventional APFC systems commonly use stepped shunt capacitors controlled by relays or contactors. Their practical behavior depends on sensor accuracy, capacitor sizing, switching delay, hysteresis, and suppression of repeated switching near decision thresholds. The present prototype adopts this stepped approach but adds Wi-Fi-based monitoring and manual control through Blynk virtual pins. The ESP8266 provides a compact 32-bit Wi-Fi-enabled controller suitable for embedded monitoring and control [9], while Blynk provides web/mobile channels for exchanging data and commands between the device and dashboards [10].

3 SYSTEM ARCHITECTURE AND PROTOTYPE CONFIGURATION

The conceptual architecture connects a single-phase 230 V, 50 Hz supply to voltage/current sensing, an ESP8266 controller, a relay module, a switched capacitor bank, and a mixed resistive-inductive load. The controller interprets the sensed state and selects the required compensation stage. Figure 1 reproduces the original block diagram.

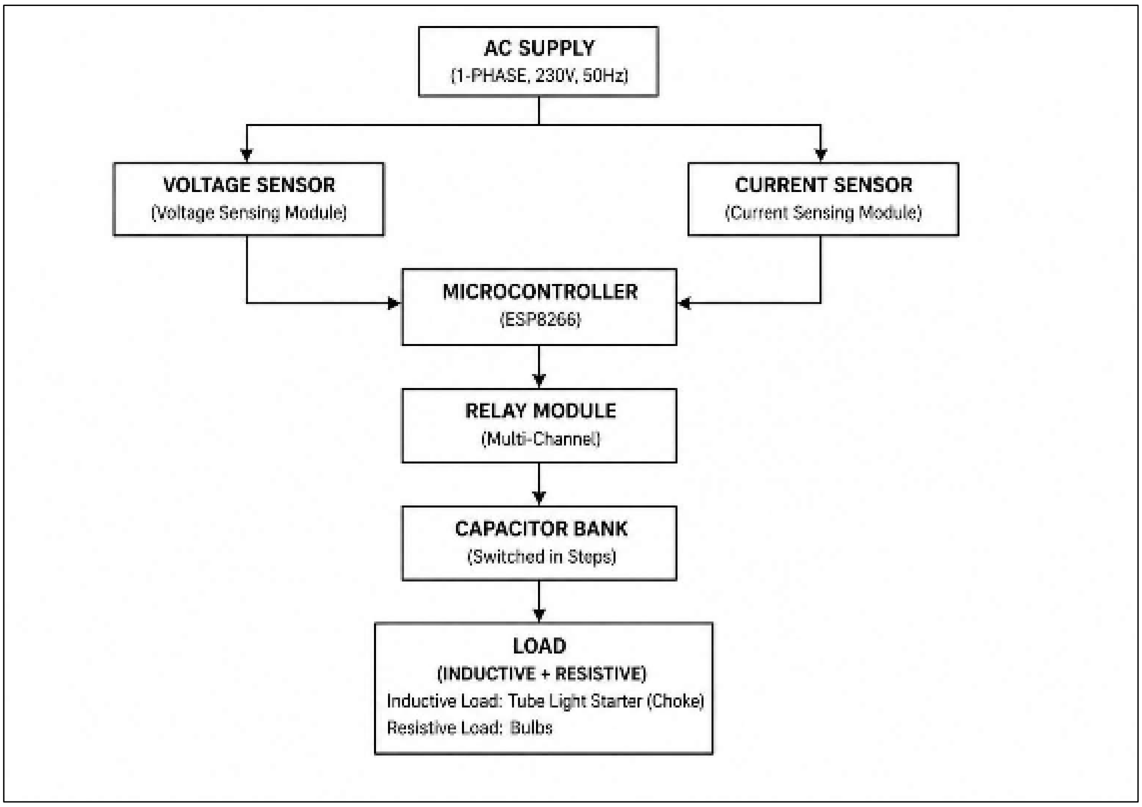

Figure 1: Original APFC block diagram.

3.1 Hardware and Loads

Table 1: Prototype hardware and source-reported specifications

Element	Specification / role
AC input	Single-phase, 230 V, 50 Hz supply
Controller	ESP8266 development board with Wi-Fi connectivity
Current sensing	ACS712 current sensor in the circuit and firmware; 185 mV/A sensitivity setting
Demonstration loads	Two 7 W LED bulbs, one 100 W incandescent bulb, and one 0-12 V step-down transformer as the inductive load
Relay interface	Active-LOW, multi-channel electromechanical relay module
Capacitor bank	Original circuit drawing shows 2.5, 4, 7.5, and 10 microfarad branches; the supplied automatic-control firmware implements two capacitor states
Local display	16 x 2 LCD, I2C address 0x27
Low-voltage supply	Regulated 5 V DC SMPS/adapter

The test loads combine nearly resistive lighting loads with a transformer used to create a lagging operating condition. Figure 2 reproduces the original resistive-versus-inductive load illustration, and Figures 3-8 retain the original component images used in the report.

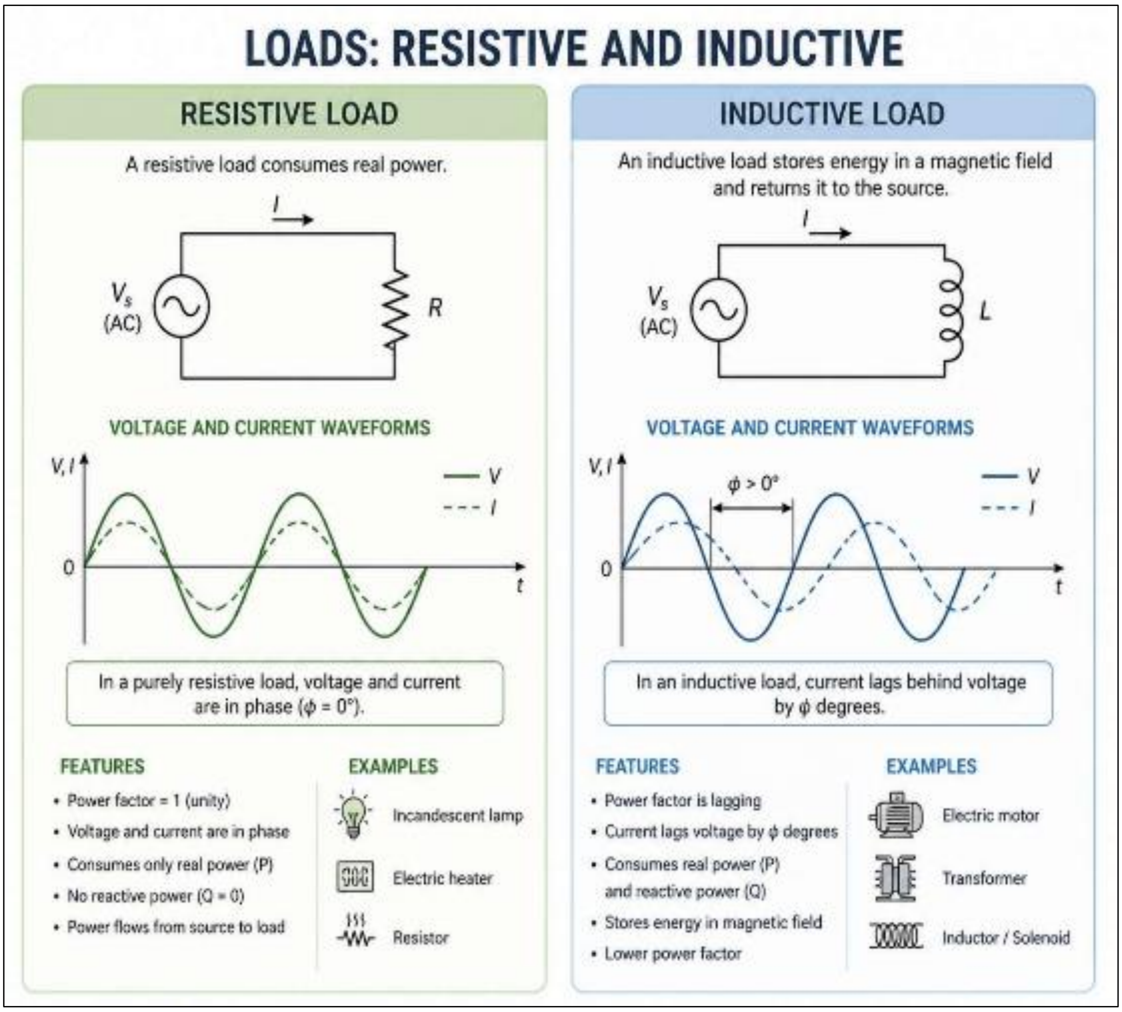

Figure 2: Original illustration of resistive and inductive load behavior

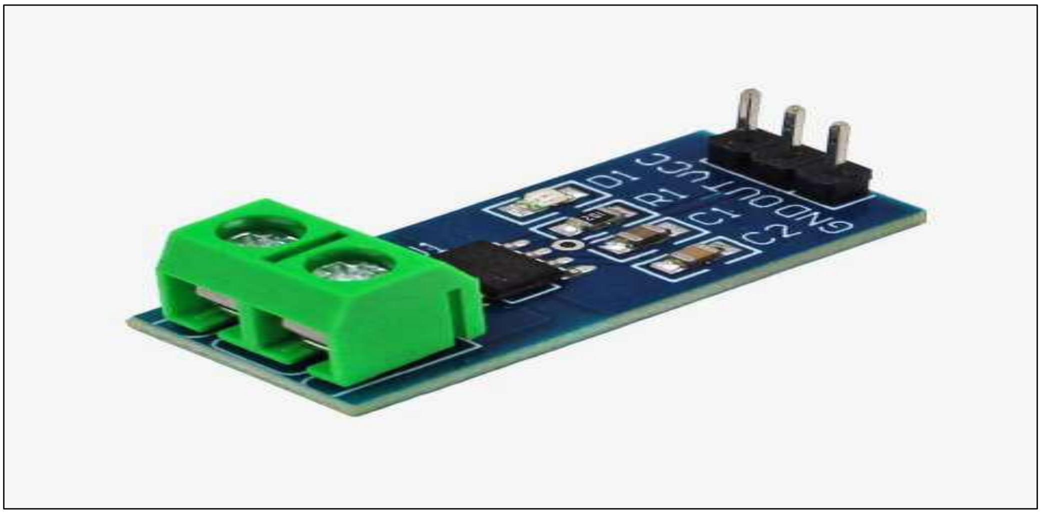

Figure 3: Original current-sensor figure

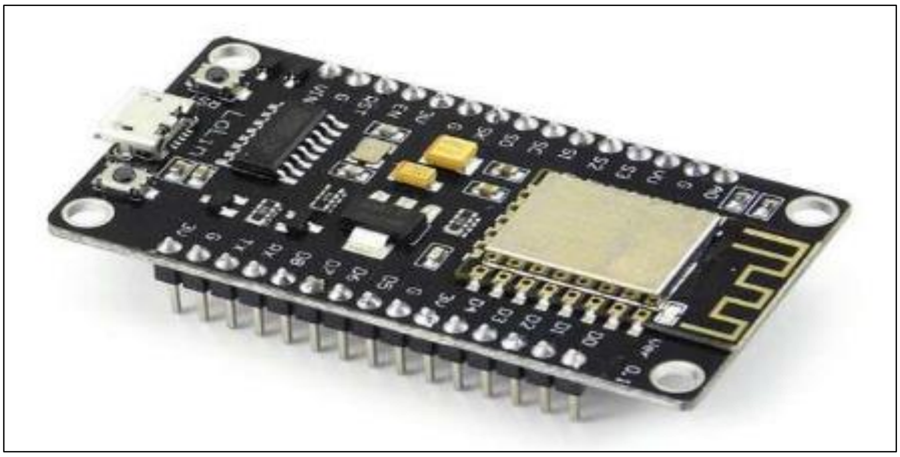

Figure 4: Original ESP8266 controller figure

Figure 5: Original relay-module figure

Figure 6: Original capacitor-bank figure

Figure 7: Original 16 x 2 LCD figure

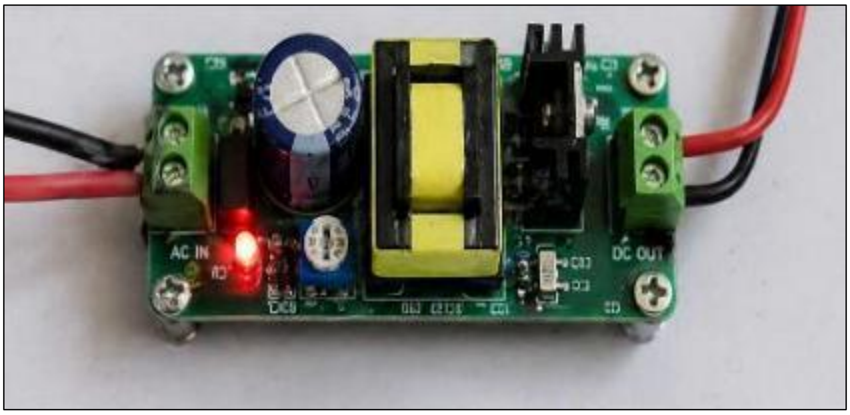

Figure 8: Original low-voltage power-supply figure

3.2 Software and IoT Interface

The controller program was developed in the Arduino environment using Embedded C/C++-style Arduino functions. The firmware uses ESP8266 Wi-Fi support, Blynk communication, Wire/I2C communication, and a LiquidCrystal_PCF8574 library. Blynk virtual pins carry the estimated power factor, current, correction status, load commands, automatic-mode command, and manual capacitor commands. The serial monitor prints current, load states, capacitor state, base power factor, corrected power factor, and the stability counter for tuning and debugging.

Table 2: Blynk virtual-pin allocation retained from the source code

Virtual pin	Function
V0	Power-factor gauge
V1	Capacitor correction/status label
V2	Current value
V3	Power-factor quality: Poor, Moderate, or Good
V5-V8	Remote load-control commands
V9	Automatic-mode command
V10-V11	Manual capacitor-stage commands

4 METHODOLOGY AND CONTROL LOGIC

4.1 Power-Factor-Correction Principle

For a sinusoidal system, power factor is defined as the ratio of active power P to apparent power S and is equal to the cosine of the voltage-current phase angle phi:

$$PF = P / S = \cos(\Phi)$$

For correction from an initial phase angle phi1 to a desired angle phi2, the required leading reactive power can be expressed as:

$$Q_c = P[\tan(\Phi_1) - \tan(\Phi_2)]$$

For a single-phase shunt capacitor at RMS voltage V and frequency f, the ideal capacitance is related to reactive power by C = Qc/(2 pi f V^2). In the prototype, fixed capacitor steps approximate the required compensation. The practical switching algorithm therefore decides when to add or remove stages rather than continuously adjusting capacitance.

4.2 Current Sampling

The firmware samples the ESP8266 analog input for 60 ms, corresponding to approximately three 50 Hz cycles. It records the peak-to-peak ADC excursion, converts it to an RMS-equivalent sensor voltage, applies the ACS712 sensitivity of 185 mV/A, and stores the result in a four-sample moving average. Readings below 0.02 A are treated as zero. This method is intended to stabilize current indication under small demonstration loads.

4.3 Firmware-Based Power-Factor Estimation

The supplied firmware does not directly sample the voltage waveform or measure phase displacement. Instead, it assigns a base power factor according to the remotely selected load combination. The transformer-only state is assigned 0.62, resistive-only operation is assigned 0.99, and mixed-load operation begins at 0.62 with increments of 0.03 for each 7 W lamp and 0.15 for the 100 W lamp, limited to 0.88 before compensation. Capacitor stage 1 adds 0.11, while the second-stage increment is 0.23; therefore, both active stages add 0.34 in the implemented getPF() function. The final value is limited to 0.99.

Table 3: Programmed power-factor model extracted from the original firmware

Load condition	Base PF	With stage 1	With stages 1 + 2
No load	1.00	Not applied	Not applied
Resistive load(s) only	0.99	Not required	Not required
Transformer only	0.62	0.73	0.96
Transformer + one 7 W lamp	0.65	0.76	0.99 (limited)
Transformer + two 7 W lamps	0.68	0.79	0.99 (limited)
Transformer + 100 W lamp	0.77	0.88	0.99 (limited)
Transformer + 100 W lamp + one 7 W lamp	0.80	0.91	0.99 (limited)
Transformer + 100 W lamp + two 7 W lamps	0.83	0.94	0.99 (limited)

4.4 Capacitor-State Machine

Automatic correction is enabled only when automatic mode is active. The controller requests stage 1 when the inductive load is on and current reaches the first threshold. Stage 2 is considered only after stage 1 has remained on for a specified settling period and the current exceeds the second threshold. A state change is accepted only after three consecutive one-second readings request the same state, reducing relay chatter. Capacitors are removed when the inductive load is off or current falls below the release threshold.

Table 4: Original switching and filtering parameters

Parameter	Value	Purpose
Minimum-load current	0.02 A	Values below this level are treated as no load
Stage-1 threshold	0.10 A	Requests first capacitor stage
Stage-2 threshold	0.40 A	Requests second stage after settling
Capacitor-off threshold	0.14 A	Provides release condition/hysteresis
Stable-reading requirement	3 consecutive readings	Prevents relay chatter
Inter-stage delay	5 s	Allows settling after first-stage switching
Control update period	1 s	Sampling, control, display, and Blynk update interval

4.5 Circuit Integration

The original circuit integrates the single-phase supply, ACS712 current sensor, ESP8266, 16 x 2 I2C LCD, relay module, parallel loads, SMPS supply, and a stepped capacitor bank. The drawing specifies capacitor branches of 2.5, 4, 7.5, and 10 microfarads. The supplied firmware, however, demonstrates two automatic capacitor-control outputs; the additional stages shown in the circuit represent an expansion path. Figure 9 reproduces the original circuit diagram without alteration.

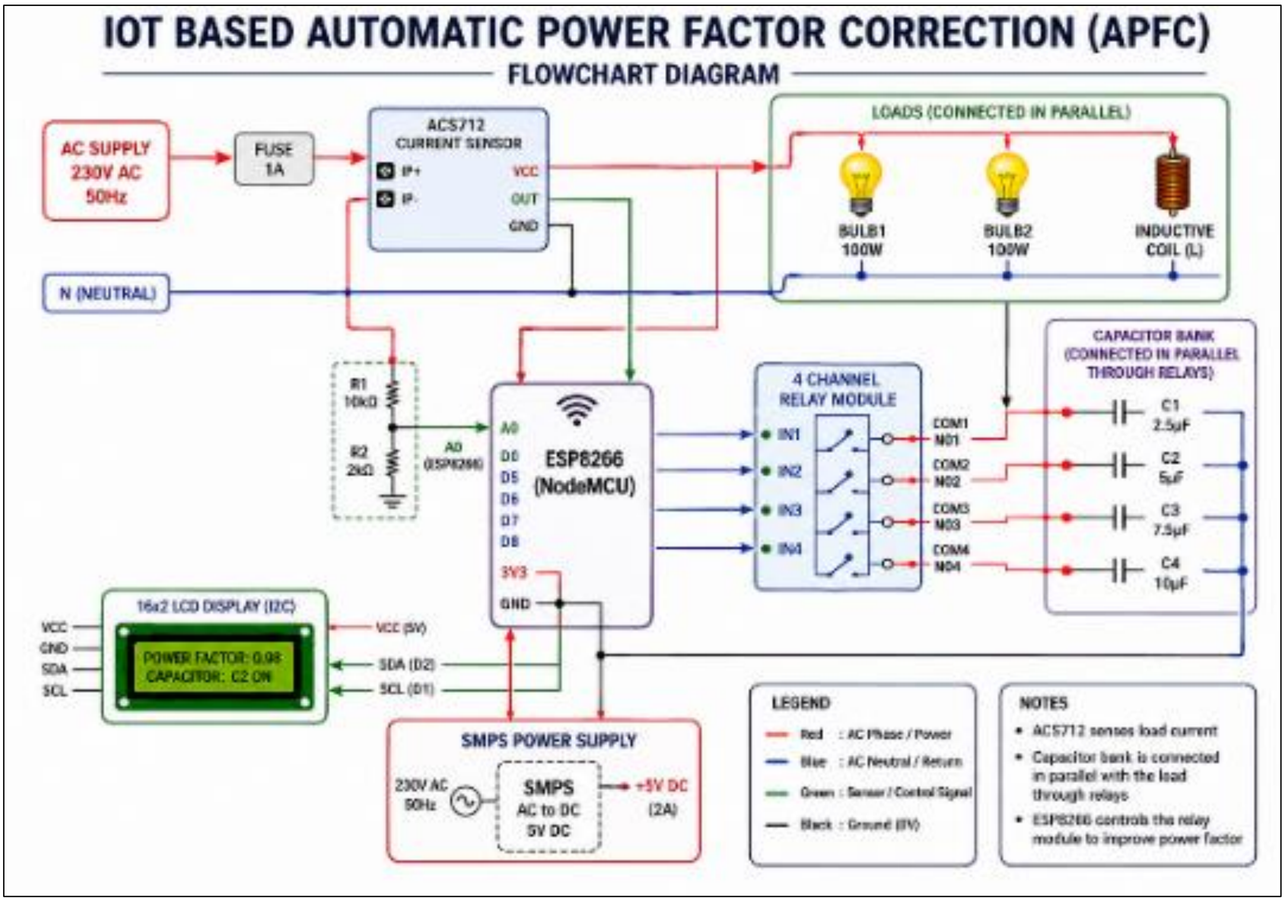

Figure 9: Original IoT-based APFC circuit diagram

5 RESULTS AND DISCUSSION

5.1 Demonstrated Operating States

The original web and mobile screenshots document two representative operating states. In the mobile view, the inductive load is on, the capacitor stages are off, the displayed current is 0.28 A, and the estimated power factor is 0.62 with a Poor classification. In the web view, the displayed current is 0.597 A, both capacitor stages are active, the reported correction is +0.34, and the estimated power factor is 0.96 with a Good classification. Because the screenshots were captured under different displayed currents and potentially different load combinations, they should be treated as separate demonstrations rather than a controlled paired before-and-after experiment.

Table 5: Values visible in the original Blynk interface screenshots

Interface/state	Current	Estimated PF	Capacitor indication	Quality
Mobile, inductive demonstration	0.28 A	0.62	OFF (+0.00)	Poor
Web, corrected demonstration	0.597 A	0.96	Cap1+2 (+0.34)	Good

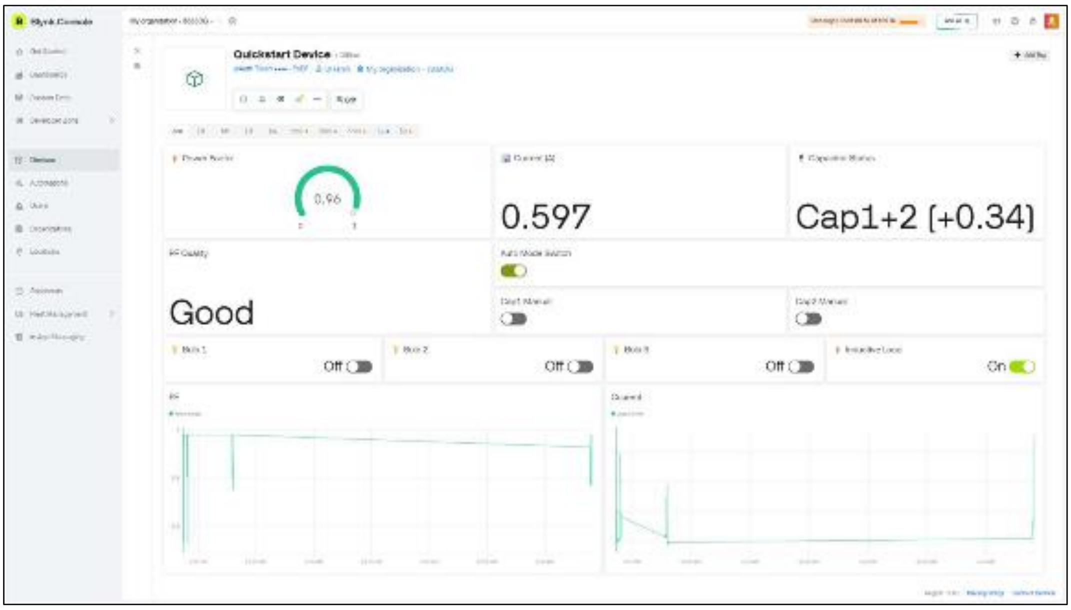

Figure 10: Original Blynk web interface showing a corrected operating state.

Figure 11: Original Blynk mobile interface showing an uncompensated inductive operating state.

5.2 Functional Assessment

The firmware structure provides several desirable control features. First, staged compensation prevents a single large correction step. Second, the stability counter and inter-stage delay reduce repeated switching and allow transient current to settle. Third, the LCD, serial monitor, and Blynk dashboards provide three independent observation channels. Fourth, automatic and manual modes support demonstration, tuning, and fault isolation. Finally, the Wi-Fi interface enables remote load control and event notifications when the estimated power factor enters low or normal ranges.

For the programmed transformer-only case, the model produces an absolute power-factor increase of 0.11 with stage 1 and 0.34 with both stages, raising the displayed value from 0.62 to 0.96. This behavior is internally consistent with the web-interface correction value of +0.34. The staged logic therefore demonstrates the intended APFC decision process and visualization workflow.

5.3 Limitations and Research Validity

The current prototype should be interpreted as an educational proof of concept rather than a metrologically validated APFC instrument. Its principal limitations are as follows:

- Power factor is estimated from known load selections and programmed constants; it is not calculated from measured real power, apparent power, or voltage-current phase angle.
- The report concept describes voltage sensing, while the supplied implementation code explicitly states that no voltage sensor or zero-crossing detector is used.
- The circuit drawing presents four capacitor branches, whereas the demonstrated automatic firmware uses two capacitor states; this should be harmonized in the next prototype revision.
- The screenshots show operating states but do not provide a controlled test matrix, calibrated reference-meter readings, uncertainty, repeated trials, line-loss measurements, or statistical analysis.
- Electromechanical relays are subject to switching delay, contact wear, and capacitor inrush current. Industrial systems require appropriately rated contactors, fuses, discharge resistors, detuning where harmonics are present, and electrical-safety compliance.

These limitations do not invalidate the educational demonstration, but they restrict claims about measured efficiency improvement, line-loss reduction, and field accuracy. A publication-grade experimental validation should compare the prototype against a calibrated power-quality analyzer over multiple load combinations and capacitor steps.

6 CONCLUSION AND FUTURE WORK

An IoT-enabled APFC prototype was organized around an ESP8266 controller, ACS712 current sensing, relay-switched capacitor stages, local LCD indication, and Blynk web/mobile supervision. The original hardware figures, circuit, interface screenshots, switching thresholds, load ratings, and programmed power-factor values have been retained. The implemented logic demonstrates staged compensation, anti-chatter confirmation, inter-stage delay, remote load control, manual override, and real-time status display. In the programmed transformer-only case, the estimated power factor changes from 0.62 to 0.96 when both capacitor stages are active.

Future development should replace load-state estimation with simultaneous voltage and current acquisition, isolated zero-crossing detection or digital phase estimation, RMS and real-power calculation, and calibration against a traceable reference instrument. The test plan should include repeated measurements for each load and capacitor state, reactive-power calculation, response time, voltage regulation, current reduction, energy-loss assessment, and uncertainty analysis. Solid-state switching or industrial contactors may be evaluated for higher-power systems. The IoT layer can be extended to cloud logging, historical trends, alarms, predictive load analysis, and smart-grid integration.

6.1 Data and Code Availability

The original project report contains the complete firmware listing and interface screenshots. For security, Wi-Fi passwords and cloud authentication tokens are not reproduced in this manuscript and should be revoked or regenerated before any public code release.

STATEMENTS ON COMPLIANCE WITH ETHICAL STANDARDS

Disclosure of conflict of interest

The authors declare no conflict of interest.

REFERENCES

[1] B. L. Theraja and A. K. Theraja, A Textbook of Electrical Technology, vol. 1. New Delhi, India: S. Chand, 2014.

[2] H. Saadat, Power System Analysis. New York, NY, USA: McGraw-Hill, 2010.

[3] I. J. Nagrath and D. P. Kothari, Modern Power System Analysis. New Delhi, India: Tata McGraw-Hill, 2003.

[4] M. H. Rashid, Power Electronics: Circuits, Devices, and Applications, 4th ed. London, U.K.: Pearson Education, 2014.

[5] B. Singh, B. N. Singh, A. Chandra, K. Al-Haddad, A. Pandey, and D. P. Kothari, "A review of single-phase improved power-quality AC–DC converters," IEEE Transactions on Industrial Electronics, vol. 50, no. 5, pp. 962–981, Oct. 2003, doi: 10.1109/TIE.2003.817609.

[6] H. Akagi, Y. Kanazawa, and A. Nabae, "Instantaneous reactive power compensators comprising switching devices without energy-storage components," IEEE Transactions on Industry Applications, vol. IA-20, no. 3, pp. 625–630, May/Jun. 1984, doi: 10.1109/TIA.1984.4504460.

[7] R. Redl and L. Balogh, "Power-factor correction in bridge and voltage-doubler rectifier circuits with inductors and capacitors," in Proceedings of the 10th Annual IEEE Applied Power Electronics Conference and Exposition, Dallas, TX, USA, 1995, pp. 466–472, doi: 10.1109/APEC.1995.468989.

[8] S. Chattopadhyay, M. Mitra, and S. Sengupta, Electric Power Quality. Dordrecht, The Netherlands: Springer, 2011, doi: 10.1007/978-94-007-0635-4.

[9] Espressif Systems, ESP8266 Technical Reference Manual, ver. 1.7, Oct. 2020.

[10] Blynk Inc., "Virtual pins and device communication," Blynk IoT Platform Documentation, accessed Aug. 3, 2026.

[11] B. Lough and B. McDonald, Power Factor Correction Circuit Basics. Dallas, TX, USA: Texas Instruments Power Supply Design Seminar, 2020.

[12] Arduino, "Arduino IDE, board-package, library, and serial-monitor documentation," Arduino Documentation, accessed Aug. 3, 2026.

[13] P. Bhagavathy, R. Latha, and E. Thamizhmaran, "Development of IoT-enabled smart APFC panel for industrial loads," in Proceedings of the 10th International Conference on Computing, Communication and Networking Technologies, Kanpur, India, 2019, pp. 1–5, doi: 10.1109/ICCCNT45670.2019.8944899.

[14] A. Cano-Ortega, F. J. Sánchez-Sutil, and J. De la Casa-Hernández, “Power factor compensation using teaching-learning-based optimization and monitoring system by cloud data logger,” Sensors, vol. 19, no. 9, Art. no. 2172, May 2019, doi: 10.3390/s19092172.

[15] S. R. Fahim, S. S. Avro, S. K. Sarker, and S. K. Das, “A novel fractional-order power-factor measurement,” SN Applied Sciences, vol. 1, no. 12, Art. no. 1611, Dec. 2019, doi: 10.1007/s42452-019-1652-4.

[16] A. J. Sari, M. A. Murti, and I. P. D. Wibawa, “Power factor correction control based on Internet of Things using lumped-compensation capacitor bank,” in Proceedings of the IEEE International Conference on Internet of Things and Intelligence Systems, Bandung, Indonesia, 2021, pp. 247–253, doi: 10.1109/IoTaIS53735.2021.9628423.

[17] M. Madhiarasan, “Design of an Internet of Things powered automated power-factor-correction system and monitoring of consumption of energy,” Wireless Personal Communications, vol. 133, no. 1, pp. 31–48, Nov. 2023, doi: 10.1007/s11277-023-10733-5.

[18] G. N. Popa and C. M. Diniș, “Low-cost system with transient reduction for automatic power-factor controller in three-phase low-voltage installations,” Energies, vol. 17, no. 6, Art. no. 1363, Mar. 2024, doi: 10.3390/en17061363.

[19] P. K. Pandey, R. Kumar, M. Singla, S. Kokin, M. Safaraliev, and J. Ahyoev, “Automated power-factor correction through microcontroller in energy sector,” Przegląd Elektrotechniczny, vol. 100, no. 10, pp. 69–72, 2024, doi: 10.15199/48.2024.10.12.

[20] C. M. Nkinyam, T. T. B. Clausel, C. Anyanwu, M. Eke, T. K. Borel, E. B. Yungho, A. Aziz, and F. Abam, “Development of a novel IoT-based monitoring and automatic power-factor-correction system for dynamic load,” Journal of Electrical Systems and Information Technology, vol. 13, Art. no. 65, Jun. 2026, doi: 10.1186/s43067-026-00371-9.